GEOPHYSICAL RESEARCH LETTERS, VOL. 29, NO. 10, 10.1029/2001GL014416, 2002

Correction published 3 March 2004

Interchange instability in the inner magnetosphere associated with geosynchronous particle flux decreases

S. Sazykin, R. A. Wolf, and R. W. Spiro
Physics and Astronomy Department, Rice University, Houston, Texas, USA

T. I. Gombosi and D. L. De Zeeuw
Department of Atmospheric, Oceanic, and Space Sciences, University of Michigan, Ann Arbor, Michigan, USA

M. F. Thomsen
Space and Atmospheric Sciences, Los Alamos National Laboratory, Los Alamos, New Mexico, USA

Received 20 November 2001; revised 15 February 2002; accepted 28 February 2002; published 28 May 2002.

[1] We simulate the inner magnetosphere during the magnetic storm of September 25, 1998 using the Rice Convection Model with boundary fluxes estimated from geosynchronous data. Model results indicate development of an interchange-like instability in the dusk-to-midnight sector, producing ripple structures in the plasma density, swirls in the subauroral ionospheric electric field pattern, and undulations near the equatorward edge of the diffuse aurora. We suggest that these disturbances might be observable whenever a strong main-phase ring-current injection is followed by a major, sustained decrease in the plasma energy density at geosynchronous orbit, a circumstance that will also produce rapid decay of the storm-time ring current. *INDEX TERMS:* 2730 Magnetospheric Physics: Magnetosphere—inner; 2736 Magnetospheric Physics: Magnetosphere/ionosphere interactions; 2772 Magnetospheric Physics: Plasma waves and instabilities; 2411 Ionosphere: Electric fields (2712)

1. Introduction

[2] Quantitative models of ring current injection require specification of the electric and magnetic fields as well as initial and boundary conditions on the particle distribution function. Two approaches have been used to model the time-dependent electric field needed for these models. In the "ring current" approach, the outer boundary is placed in the range 6.6–10 R_E with analytic expressions specifying the time dependent electric potential. The first of these models appeared long ago [e.g., *McIlwain*, 1974], with later versions [e.g., *Liemohn et al.*, 2001; *Fok et al.*, 2001] including sophisticated representations of loss processes. The second (or "convection model") approach computes the potential electric field self-consistently by explicitly considering coupling between the magnetospheric plasma and the conducting ionosphere. The best known of these models, the Rice Convection Model (RCM) [e.g., *Harel et al.*, 1981], generally places the nightside boundary far enough away from the Earth (12–20 R_E) to include most of the region-2 (shielding) Birkeland currents. Typically, the RCM particle flux boundary conditions are estimated using statistical plasma-sheet models and are held constant through a run. This approach with the RCM has been used to model ring-current injections [*Wolf et al.*, 1982; *Garner*, 2000].

[3] Recently, we have begun using convection models in "ring current" mode, i.e., with the outer boundary set close to Earth and the particle boundary condition varied in time [*Fok et al.*, 2001]. Here we describe results for the magnetic storm of September 25, 1998 with the outer boundary set at $L = 6.6$ and the particle boundary condition following time variations suggested by geosynchronous spacecraft. Results exhibit an interchange-type instability that has not appeared in previous published RCM simulations, though the possibility of such an instability was suggested many years ago [e.g., *Gold*, 1959; *Sonnerup and Laird*, 1963].

0094-8276/02/2001GL014416

2. Run Setup and Inputs

[4] Since RCM algorithms are described elsewhere [e.g., *Harel et al.*, 1981; *Wolf et al.*, 1991], we give only run-specific details here. Outer and inner boundaries are set at $L = 6.6$ and $L = 1.01$, respectively. The plasma population is represented by 75 proton and 25 electron isotropic "fluids" with energy invariants λ_s and flux-tube content η_s related to the energy W_s and number density n_s through the flux-tube volume $V = \int ds/B$:

$$\lambda_s = W_s V^{2/3};\ \eta_s = n_s V. \tag{1}$$

The RCM advects each fluid using:

$$\left[\frac{\partial}{\partial t} + \frac{\vec{B} \times \nabla\left(\Phi + (\lambda_s/q_s)V^{-2/3}\right)}{B^2} \cdot \nabla\right] \eta_s = -L, \tag{2}$$

where Φ is the electric potential in an inertial frame, and L represents losses. Φ is found by solving the Vasyliunas equation:

$$\nabla \cdot \left(-\hat{\Sigma} \cdot \nabla(\Phi - \Phi_c)\right) = \hat{b} \cdot \nabla V \times \nabla P, \tag{3}$$

where Φ_c transforms to the rotating ionospheric frame, operator ∇ acts on the ionospheric spherical shell, $\hat{\Sigma}$ is a 2×2 conductance tensor, and $\hat{b}$ is a unit magnetic field vector (assumed to be dipolar for this run).

[5] The potential on the poleward boundary is taken from the *Maynard and Chen* [1975] *Kp*-dependent model. Ion losses in (2) are assumed due to charge-exchange only. Plasma loss by convection through the dayside magnetopause [*Liemohn et al.*, 2001] is implicit in the RCM solution of (2). Solar-EUV-generated conductances are estimated from the IRI-90 empirical ionosphere; atmospheric dynamo electric fields are not included. Electron precipitation is assumed to be 30% of the strong-pitch-angle-scattering limit. The average energy and flux of precipitating electrons are computed from the distribution of plasma sheet electrons as in *Wolf et al.* [1991], and auroral conductances are then estimated according to *Robinson et al.* [1987]. Field-aligned potential drops are neglected.

[6] We have replaced the usual RCM Lagrangian algorithm for solving (2) with a new grid-based advection scheme based on multi-dimensional wave propagation methods. This allows the boundary plasma condition to be easily changed in time to reflect measured fluxes. The ability of this new algorithm to track sharp discontinuities in η is crucial to modeling interchange instabilities.

[7] Variable plasma fluxes at $L = 6.6$ are set from measured Magnetospheric Plasma Analyzer (MPA) moments for $E < 50$ keV [*Thomsen et al.*, 1996] in a way similar to that used by kinetic ring-current models [e.g., *Liemohn et al.*, 2001]. The temperatures are assumed to represent particles with kappa distributions ($\kappa = 6$). Nighttime η boundary values are extended in local time, with the largest values used if data from multiple spacecraft are available. In the calculation of η's from measured fluxes, ions are assumed to be protons.

[8] Figure 1 shows measured moments and geomagnetic indices for the magnetic storm of September 25, 1998. In this storm, *Dst* recovers quickly (within half a day) from its minimum value of −200 nT. Data within 4 hours MLT of midnight were used to generate the curves in Figure 1; when no data were available, idealized step-wise approximations were used. Note that P varies by more than a factor of 4 over the course of the magnetic storm. Geosynchronous pressure increases are typically associated with enhanced magnetospheric convection and ring current injection. It is less clear why the measured fluxes dropped some time around 09 UT on September 25, but similar observations exist for other magnetic storms.

3. Model Predictions and Discussion

[9] Plate 1 shows four "snapshots" of a significant interchange instability event that occurred in the simulation following a large drop in charged particle flux at geosynchronous orbit at 09 UT on September 25.

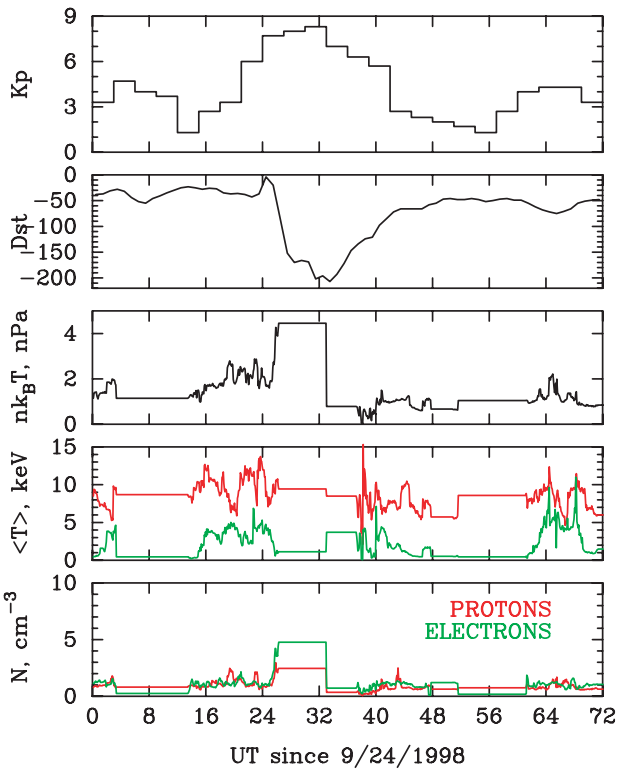

Figure 1. *Kp*, *Dst* indices, measured plasma moments, and total plasma pressure.

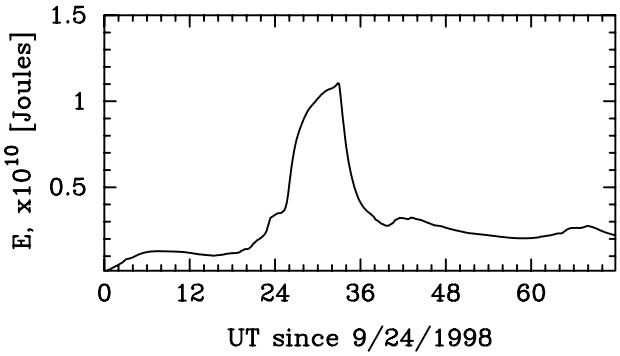

Plate 1. Total particle energy in the region $L < 6.6$.

[10] In the ideal MHD approximation, the interchange instability has been extensively discussed, for example, by *Schmidt* [1979], who showed that a static-equilibrium configuration is interchange unstable if there exist two adjacent flux tubes of unit magnetic flux, with pressure P and flux-tube volume V and $(P + \delta P, V + \delta V)$ respectively, such that

$$\delta V \cdot \delta\left(PV^{5/3}\right) < 0. \tag{4}$$

Usually, within the magnetosphere, both V and $PV^{5/3}$ increase outward, and the system is stable. However, a decrease in the boundary value of $PV^{5/3}$ with time naturally injects flux tubes with low values of $PV^{5/3}$ into a region of larger V, outside of higher-$PV^{5/3}$ tubes.

[11] The equatorial potential pattern at 09:10 UT shows strong outward-directed electric field in the dusk-to-midnight sector. This feature, typical of simulations of strong magnetic storms [e.g., *Garner*, 2000], has also been seen in CRRES electric field observations [*Rowland and Wygant*, 1998]. However, the η pattern at 09:10 UT contains the seeds of interchange instability. High-$PV^{5/3}$ flux tubes injected earlier form an essentially complete ring (the storm-time ring current). When $PV^{5/3}$ decreases at the boundary, lower-content plasma enters the nightside modeling region, resulting in an unstable interchange disruption that is obvious at subsequent times on Plate 1. Thick fingers of high-$PV^{5/3}$ plasma move outward, their positions in the ring taken by low-$PV^{5/3}$ plasma. As the interchange occurs, the fingers also drift to the west. In accordance with (2) and (3), gradients in $PV^{5/3}$ create strong electric fields, which are seen as ripples and swirls in the potential contours.

[12] The right column of Plate 1 illustrates the relationship between disturbance electric fields and the auroral conductances. As the interchange develops, perturbation electric fields affect, in a self-consistent way, the drifts of electrons as well as ions, resulting in pre-midnight undulations of the diffuse aurora. The electric field swirls are centered just equatorward of the diffuse aurora, but they sometimes penetrate into the auroral zone. Another important effect of this instability is rapid loss of the storm-time ring current. The interchange process immediately decreases particle energy, because particles in the high-content tubes adiabatically lose energy as they move out. Also, many of those high-content tubes move from closed, Earth-circling trajectories to open drift paths that exit through the dayside magnetopause. In this way, interchange enhances the loss-through-magnetopause mechanism [e.g., *Liemohn et al.*, 2001].

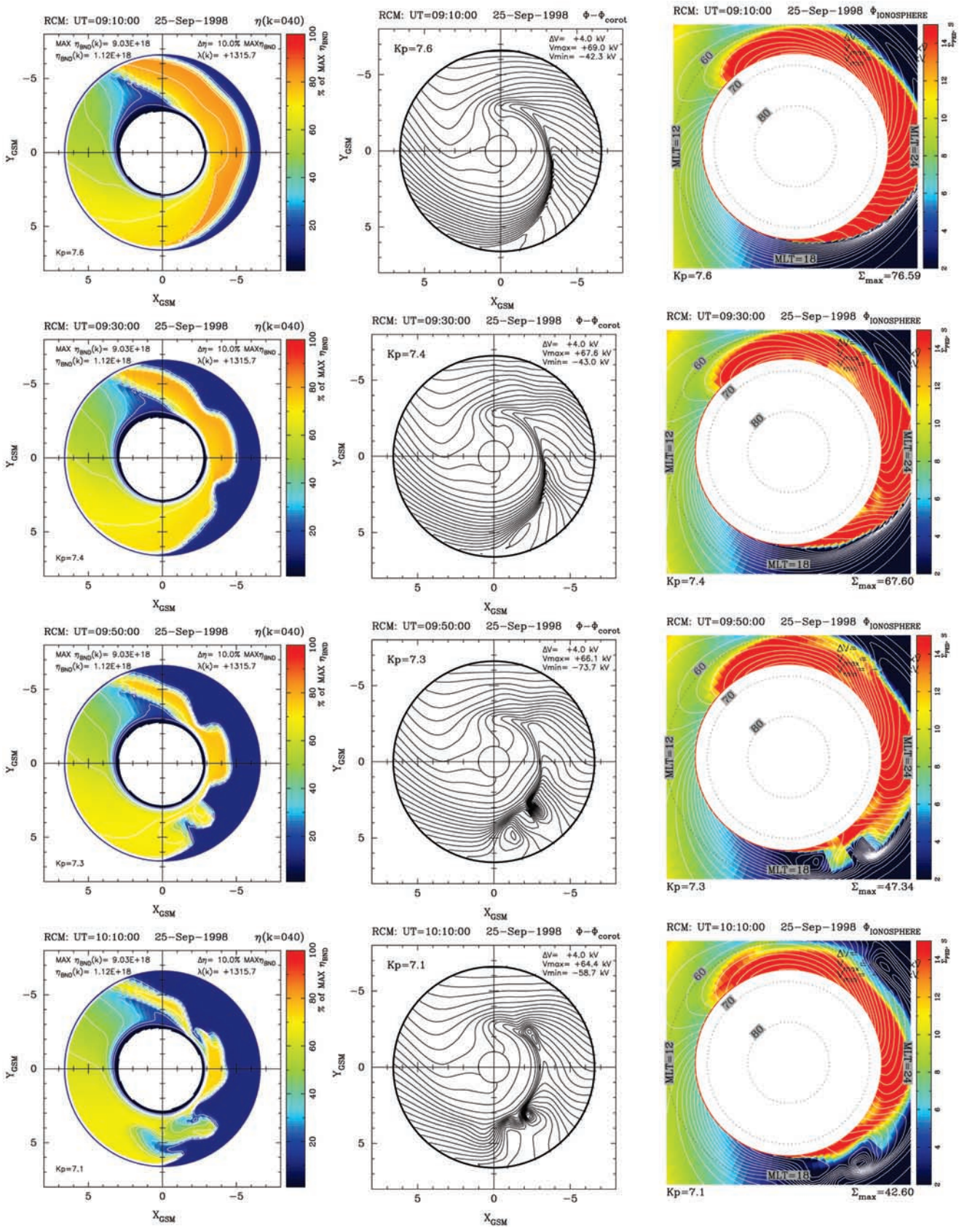

Figure 2. Plasma densities, electric potential, and conductances during an interchange event. Snapshots are shown four times on September 25. Sun is to the left. Left column, flux-tube content η for protons with $\lambda = 1316$, corresponding to 9 keV at $L = 6.6$ (equat. view); middle column, electric potential (equat. view); right column, potential (contours) and Pedersen conductance in the ionosphere. On the nightside, regions of high conductance correspond to the diffuse aurora.

Figure 2 shows that the total particle energy decreases rapidly after the interchange instability takes hold.

[13] We should note that contrary to the assumptions of the ideal MHD energy principle analysis, the inner magnetosphere is not in pure static equilibrium, but is undergoing slow flow. Also, the frozen-in-flux condition is violated since gradient and curvature drift is comparable to $\vec{E} \times \vec{B}$ drifts, causing different plasma components to drift at different velocities. These effects act to decrease the growth rate of the instability. As a consequence, the RCM shows noticeable interchange instability behavior only when the decrease in $PV^{5/3}$ at the boundary is substantial and sustained. Also, the finite-grid resolution of the RCM (0.2° in latitude and 0.25 hr in MLT) considerably slows the growth of interchange ripples with wavelengths of only a few grid spaces.

[14] Using the measured MPA moments in the manner indicated probably led us to underestimate the RCM's boundary-condition ion fluxes, for two reasons. The 50-keV energy cutoff of the MPA artificially reduced density and temperature, and interpreting measured ions as protons probably resulted in a further underestimate of density, because of the high concentrations of oxygen typically observed in major storms [*Daglis et al.*, 1999]. Another RCM run assuming four times higher boundary density and 1.75 times higher ion temperature showed modestly stronger interchange effects than those shown in Plate 1.

[15] Large-scale undulations associated with the equatorward edge of the diffuse aurora have previously been reported from DMSP photographs by *Lui et al.* [1982], who interpreted the undulations as due to Kelvin-Helmholtz instability during strong subauroral ion drift (SAID) events [*Kelley*, 1986; *Yamamoto et al.*, 1994]. The ''giant'' wave-like structures of *Lui et al.* [1982] displayed wavelengths of 200–900 km, smaller than the interchange ripples found in our simulations. However, our grid spacing does not allow smaller-scale structures to be resolved.

[16] To conclude, the RCM consistently showed highly structured electric field and plasma density perturbations in the inner magnetosphere associated with large, quick, and sustained drops in plasma fluxes measured by Los Alamos particle detectors on geosynchronous satellites. Based on the physical picture that emerges from the simulations, we expect interchange to last a few hours whenever nightside geo ion fluxes show major, sustained declines following the injection of a main phase ring current. The flux decreases must occur on quasi-dipolar field lines, earthward of the central plasma sheet, not on field lines that extend to the tail lobes. The result may be a rapid decay of the storm-time ring current and a rapid recovery of *Dst* back toward normal levels. In the right circumstances and for magnetic storms with a quick *Dst* recovery, we expect the interchange events to be observable in spacecraft auroral imagery and in nightside electric field observations from the Millstone Hill incoherent-backscatter radar. Observations taken September 25, 1998 by the incoherent radar at Irkutsk, Russia indicate occurence of quasi-periodic electric field disturbances nearly co-located (temporarily and spatially) with model-predicted interchange disturbances (J. Foster, private communication), and will be the subject of a separate study.

[17] **Acknowledgments.** The authors are grateful to Janet Kozyra for suggesting this RCM run. The work was supported by the NASA Sun-Earth-Connection Theory Program under grant NAG5-8136 to Rice University, and by NSF KDI grant ATM-9980078 to the University of Michigan (with subcontract to Rice).

References

Daglis, I. A., R. M. Thorne, W. Baumjohann, and S. Orsini, The terrestrial ring current: Origin, formation and decay, *Rev. Geophys.*, *37*, 407–438, 1999.

Fok, M.-C., R. A. Wolf, R. W. Spiro, and T. E. Moore, Comprehensive computational model of Earth's ring current, *J. Geophys. Res.*, *106*, 8417–8424, 2001.

Garner, T. W., A case study of the June 4–5, 1991 magnetic storm using the Rice Convection Model, Ph.D. thesis, Rice University, Houston, Texas, 2000.

Gold, T., Motions in the magnetosphere of the Earth, *J. Geophys. Res.*, *64*, 1219–1224, 1959.

Harel, M., R. A. Wolf, P. H. Reiff, R. W. Spiro, W. J. Burke, F. J. Rich, and M. Smiddy, Quantitative simulation of a magnetospheric substorm 1, Model logic and overview, *J. Geophys. Res.*, *86*, 2217–2241, 1981.

Kelley, M. C., Intense sheared flow as the origin of large-scale undulations of the edge of the diffuse aurora, *J. Geophys. Res.*, *91*, 3225–3230, 1986.

Liemohn, M. W., J. U. Kozyra, M. F. Thomsen, J. L. Roeder, G. Lu, J. E. Borovsky, and T. E. Cayton, Dominant role of the asymmetric ring current in producing the stormtime Dst, *J. Geophys. Res.*, *106*, 10,883, 2001.

Lui, A. T. Y., C.-I. Meng, and S. Ismail, Large-amplitude undulations on the equatorward boundary of the diffuse aurora, *J. Geophys. Res.*, *87*, 2385, 1982.

McIlwain, C. E., Substorm injection boundaries, in *Magnetospheric Physics*, edited by B. M. McCormac, pp. 143–154, D. Reidel, Dordrecht-Holland, 1974.

Maynard, N. C., and A. J. Chen, Isolated cold plasma regions: Observations and their relation to possible production mechanisms, *J. Geophys. Res.*, *80*, 1009–1013, 1975.

Robinson, R. M., R. R. Vondrak, K. Miller, T. Dabbs, and D. Hardy, On calculating ionospheric conductances from the flux and energy of precipitating electrons, *J. Geophys. Res.*, *92*, 2565, 1987.

Rowland, D. E., and J. R. Wygant, Dependence of the large-scale, inner magnetospheric electric field on geomagnetic activity, *J. Geophys. Res.*, *103*, 14,959–14,964, 1998.

Schmidt, G., *Physics of High Temperature Plasmas*, Academic Press, New York, 1979.

Sonnerup, B. U. Ö., and M. J. Laird, On the magnetospheric interchange instability, *J. Geophys. Res.*, *68*, 131–139, 1963.

Thomsen, M. F., D. J. McComas, G. D. Reeves, and L. A. Weiss, An observational test of the Tsyganenko (T89a) model of the magnetospheric field, *J. Geophys. Res.*, *101*, 24,827, 1996.

Wolf, R. A., M. Harel, R. W. Spiro, G.-H. Voigt, P. H. Reiff, and C. K. Chen, Computer simulation of inner magnetospheric dynamics for the magnetic storm of July 29, 1977, *J. Geophys. Res.*, *87*, 5949–5962, 1982.

Wolf, R. A., R. W. Spiro, and F. J. Rich, Extension of convection modeling into the high-latitude ionosphere: Some theoretical difficulties, *J. Atmos. Terr. Phys.*, *53*, 817, 1991.

Yamamoto, T., M. Ozaki, S. Inoue, K. Makita, and C.-I. Meng, Convective generation of ''giant'' undulations on the evening diffuse auroral boundary, *J. Geophys. Res.*, *99*, 19,499, 1994.

S. Sazykin, R. W. Spiro, and R. A. Wolf, Physics and Astronomy Department, MS-108, Rice University, Houston, TX 77005-1892, USA. (sazykin@rice.edu; wolf@alfven.rice.edu; spiro@rice.edu)

T. I. Gombosi and D. L. De Zeeuw, Department of Atmospheric, Oceanic, and Space Sciences, University of Michigan, Ann Arbor, MI 48109-2143, USA.

M. F. Thomsen, Space and Atmospheric Sciences (NIS-1), Los Alamos National Laboratory, Los Alamos, NM 87545, USA.